iScience

CellPress
OPEN ACCESS

Article

Effect of THz spectra of L-Arginine molecules by the combination of water molecules

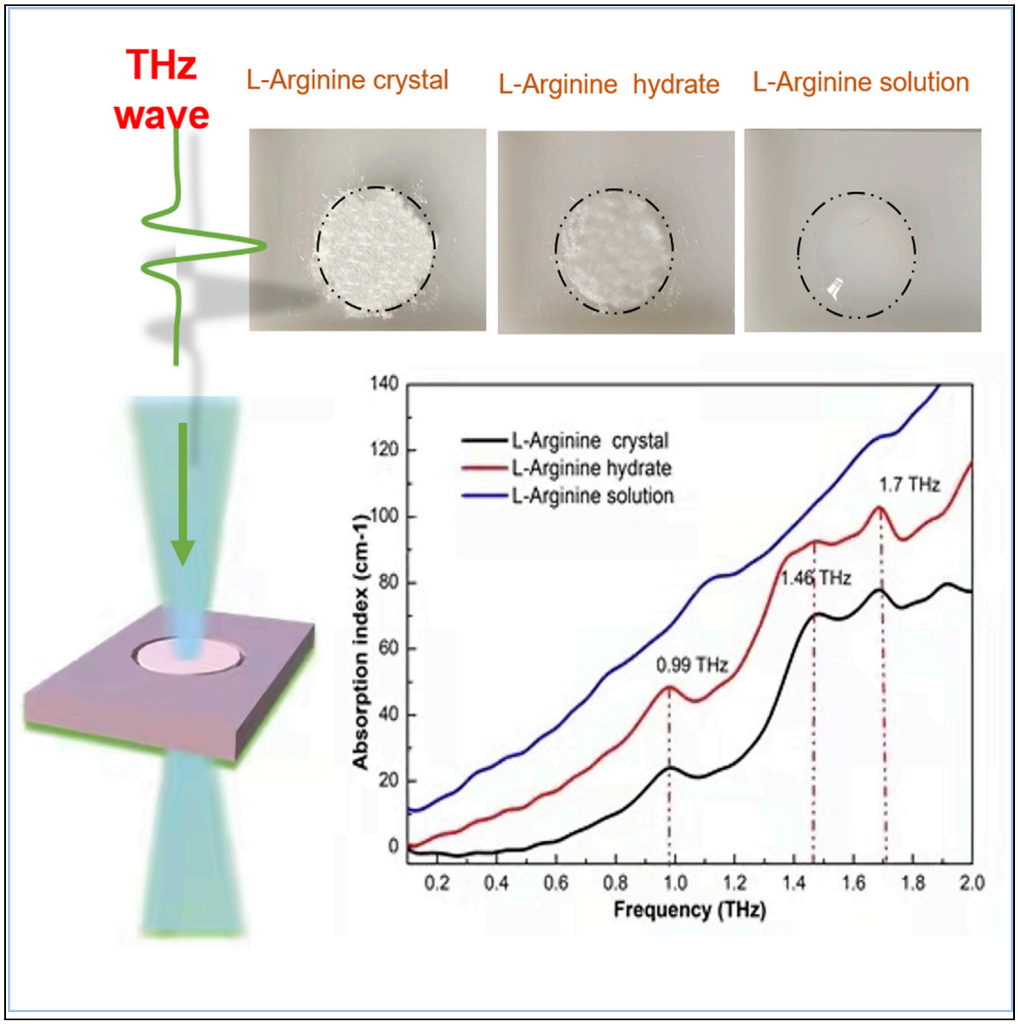

Haiqing Wang, Wei Shi, Lei Hou, Zhiquan Wang, Meilin Wu, Chaofan Li, Chunhui Li

swshi@mail.xaut.edu.cn (W.S.)
houleixaut@126.com (L.H.)

Highlights

L-Arginine crystal and its hydrate have the same three absorption peaks

L-Arginine solution and free water have the same trend of absorption spectra

The increment of water volume in the sample, the absorption baseline is rising

Wang et al., iScience 25, 103788
February 18, 2022
https://doi.org/10.1016/j.isci.2022.103788

iScience

CellPress
OPEN ACCESS

Article

Effect of THz spectra of L-Arginine molecules by the combination of water molecules

Haiqing Wang,[1] Wei Shi,[1,*] Lei Hou,[1,*] Zhiquan Wang,[1] Meilin Wu,[1] Chaofan Li,[1] and Chunhui Li[1]

SUMMARY

Most biomolecules are biologically active only in water; hence, it is worth investigating whether THz spectra of biomolecules are affected by the combination of water molecules and biomolecules. In this report, by combining the sample cell with the THz-TDS system, the THz spectra of L-Arginine crystal as well as its hydrate and aqueous solution are measured. The experimental results show that L-Arginine crystal and its hydrate share the same three absorption peaks at 0.99, 1.46, and 1.7 THz, respectively. But the trend of characteristic absorption spectrum of L-arginine solution is almost identical to that of free water. Because the contents of free water and hydrated water are different in many diseased and normal tissues, the diseased tissues can be detected according to the difference in THz spectral information. The proposed approach provides a reliable means for the detection of pathological changes of active molecules and tissues.

INTRODUCTION

Terahertz (THz) technology is of great significance in organisms, biological macromolecules, nucleic acids, proteins, and sugars because it can provide the information that usually cannot be obtained directly through detection methods of optical, X-ray, and nuclear magnetic resonance (Peng et al., 2020; Liu et al., 2019; Zhu et al., 2021). To date, the THz method has been successfully applied to molecular and cell biology (Shi et al., 2020; Penkov and Fesenko, 2020; Nagai et al., 2005; Wang et al., 2021). However, most of these existing works focus on solid anhydrous substance, whereas aqueous solutions are rarely studied. One main reason for this is that the strong absorption of THz waves by water masks the absorption of dissolved substances (Markelz et al., 2000).

L-Arginine is an essential amino that plays an irreplaceable role in the life metabolism (Biman and Bagchi, 2005). Therefore, it is particularly important to study the biophysical properties of L-Arginine. Note that biomolecules exist in the aqueous environment, so all functions of proteins are realized through the interaction between molecules and surrounding solvent molecules (Bagchi, 2005). Owing to the large electric dipole moment of water, a hydrated layer is easily formed by the strong interaction with the surface charges of biomolecules (Doan and Vinh, 2020). Such a layer of water molecules is also referred to as hydration water, as it envelops a biomolecule and its physical properties are different from that of bulk water. From a molecular viewpoint, the spectral differences between normal and diseased tissues mainly come from the differences in the contents of free water and hydrated water in diseased molecules (Pickwell et al., 2004; Woodward et al., 2002). In recent years, although analysis the THz characteristics of biomolecules, hydrated water around biomolecules, and bulk water of hydration sensitive diseases is receiving increasing attention, the hydrodynamics of hydrated water and dispersed water on biomolecules is not well studied (Gupta et al., 2019; Heugen et al., 2006). To solve this issue, several methods for detecting THz spectra of hydrated biological samples have been developed, including the utilization of THz attenuated total reflection (THz-ATR) (Tang et al., 2020; Yi et al., 2017), microfluidic chips (Yang et al., 2018), and metamaterial sensors (Xu et al., 2016; Zhang et al., 2016). However, these methods are not used widely because of their relatively poor operability, integration limitations, and high cost. Recently, our team designed a horn-shaped tapered parallel plate waveguide (HSTPPW), which can enhance the electrical field of the incident THz wave at its central position (Hou et al., 2021; Shi et al., 2021). Based on HSTPPW, the THz spectral information of substances in an aqueous solution can be obtained by the THz time-domain spectroscopy (THz-TDS) system with high accuracy, although the method is expensive and it is a little difficult to control the thickness of the sample dropped into the waveguide.

By combining the sample cell with the THz-TDS system, THz spectra of the L-Arginine molecule from crystalline to dissolved state were measured. We obtain the spectral characteristics of three kinds of L-Arginine

[1]Key Laboratory of Ultrafast Photoelectric Technology and Terahertz Science in Shaanxi, Xi'an University of Technology, Xi'an 710048, China

*Correspondence: swshi@mail.xaut.edu.cn (W.S.), houleixaut@126.com (L.H.)

https://doi.org/10.1016/j.isci.2022.103788

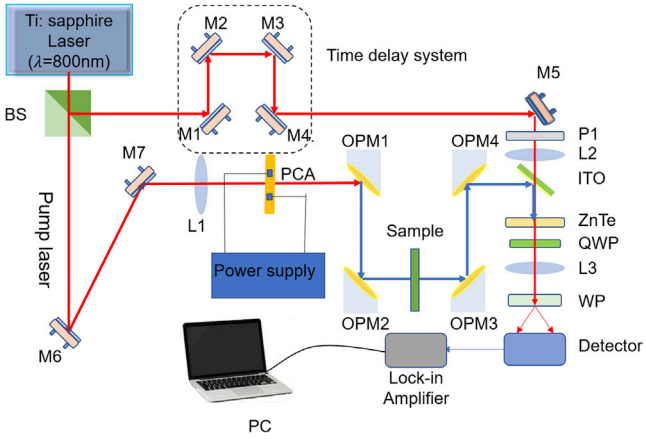

Figure 1. Experimental setup of terahertz measurement system based on antenna

BS, beam splitter; PCA, photoconductive antenna; OPM, off-axis parabolic mirror; P, polarizer; M, mirror; ITO, indium tin oxide; QWP, quarter waveplate; WP, Wollaston prism, L: lens.

samples in THz frequency. Compared with the existing THz spectroscopy detection methods of aqueous biological samples based on HSTPPW, the direct detection method of sample cell is relatively simple and cost-effective. Of importance, it provides a possibility for disease detection and drug screening at a molecular level in the future.

RESULTS AND DISCUSSION

Terahertz spectrum

We have built a THz-TDS system, and its overall optical path is shown in Figure 1. In the experiment, the ambient temperature was 25°C and the THz-TDS system was purged by dry air to ensure that the relative humidity in the system was kept at about 3%. Before detecting the biological sample, we used a push-pull methyl pentene copolymer (commonly referred to as TPX) sample cell and prepared three types of samples involving L-Arginine. The specific process is shown in Figure 2. The empty TPX sample cell was placed at the focus of OPM2 (off-axis parabolic mirror 2) for generating and recording a *reference signal*. Compared with the transmission rates of the empty sample cell and air, the TPX material is almost transparent in the THz band, mainly due to its nonpolar and amorphous material structure. The dry tablet, suspension, and dissolved solution of L-Arginine were measured and recorded as *L-Arginine crystal*, *L-Arginine hydrate*, and *L-Arginine solution*, respectively.

Figure 3A shows the time-domain waveforms of the reference signal, L-Arginine crystal, L-Arginine hydrate, and L-Arginine solution. Compared with the reference signal of the empty sample cell, the signal of the three L-Arginine samples has an obvious time delay effect that is caused by refraction of the THz wave through the samples. Meanwhile, it is observed from Figure 3A that, under the same thickness, the more the volume of water contained in the sample, the more obvious the time delay effect is. When the water volume in the sample increases, the amplitude of the time-domain waveform decreases correspondingly. This reveals that the absorption of THz wave increases with the increase of water.

Furthermore, Figure 3B shows the frequency spectra of the reference and three samples obtained by fast Fourier transform. From the spectra, we find that the bandwidth of the reference signal is about 3 THz; after being attenuated by the sample, the bandwidth is only 2 THz. Therefore, we only discuss the spectral characteristics of the sample between 0.1 and 2 THz. The amplitude of L-Arginine crystal is nearly equivalent to that of the reference before 0.5 THz but drops significantly between 0.5 and 2 THz. Besides, the drop of amplitude is obvious at a fixed frequency, i.e., there exists an absorption peak. In particular, the spectrum amplitude of L-Arginine hydrate decreases sharply from 0.1 to 2 THz. L-Arginine hydrate has an amplitude drop at the same frequency as that of L-Arginine crystal. However, the spectral amplitude of L-arginine solution decreased more quickly than that of its crystal and hydrate. At the same time, the amplitude of L-Arginine solution had no obvious drop in the peak frequency.

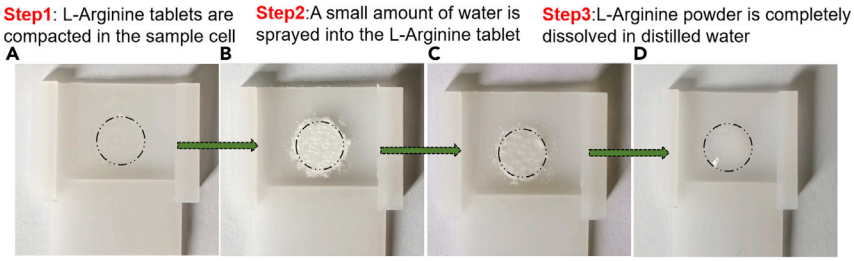

Figure 2. Photos of push-pull methyl pentene copolymer (commonly referred to as TPX) sample cell and preparation process of three types of samples involving L-Arginine

(A–D) Empty sample cell (its inner diameter and depth are 7 mm and 100 μm, respectively); (B) dry anhydrous L-Arginine tablets; (C) L-Arginine suspension; and (D) L-Arginine solution.

Absorption coefficient and refractive index

THz waves are attenuated by the dielectric medium because of the absorption of the sample cell and L-Arginine samples; thus, the absorption coefficient of the sample is obtained by subtracting the influence of the sample cell. According to Beer-Lambert's law, after subtracting the contribution from the background signal (usually the reference signal), the absorption coefficient of the L-Arginine sample is calculated as

$$\alpha(\omega) = -\log_{10}(A(\omega)/A_0(\omega))/(d_2 - d_1)$$

where $d_2 - d_1$ = 100 μm is the thickness of the sample cell and $A_0(\omega)$ and $A(\omega)$ is the amplitude of the reference and L-Arginine samples at the frequency of ω, respectively.

According to Equation 7, we can obtain the characteristic absorption spectra of L-Arginine crystal, L-Arginine hydrate, and L-Arginine solution. The results are illustrated in Figure 4A. It can be seen that L-Arginine crystal and L-Arginine hydrate share the same three absorption peaks at 0.99, 1.46, and 1.7 THz, respectively, in the range from 0.1 to 2.0 THz. But L-Arginine solution and free water share the same trend of characteristic absorption spectrum. In addition, we find that the absorption baselines of the three L-Arginine samples are different.

Moreover, note that, in the low-frequency region below 0.5 THz, L-Arginine crystal has no absorption but the baselines of L-Arginine hydrate and solution are significantly higher than that of L-Arginine crystal. In the range of 0.5–2 THz, L-Arginine crystal and its hydrate share the same three absorption peaks at 0.99, 1.46, and 1.7 THz, respectively. However, L-Arginine solution has no obvious absorption peak in the range of 0.5–2 THz. This indicates that, with the increment of water volume in the sample, the corresponding absorption baseline rises. Herein, it is inferred that the absorption baseline rises because of the strong absorption of water in the detectable frequency range.

We continued to analyze the absorption spectrum of each sample separately. It was observed that L-Arginine crystal has distinct absorption peaks at some fixed frequency. However, L-Arginine solution has no similar peaks, but its absorption trend is nearly the same as that of free water. The absorption spectrum of L-Arginine hydrate not only shares the same absorption peaks at a fixed frequency but also has the absorption spectrum characteristics of free water. We infer that these phenomena may be caused by the following reasons. First, the three absorption peaks of L-Arginine crystal are caused by the vibration of the low-frequency molecule itself. Second, after we add water to the L-Arginine tablet, the hydration layer is formed around the solute owing to electrostatic action and hydrogen bonding. As the hydration layer tightly covers the surface of the L-Arginine molecule, its hydrodynamic surface will decrease the THz absorption. In addition, the molecular structure of L-Arginine cannot form a monohydrate with water molecules, and the polarity of the molecule and the interaction force between the molecules will not change correspondingly; hence, there is no new absorption peak. These explain why the absorption spectrum of L-Arginine hydrate has the absorption peak of the sample and the absorption characteristics of the hydration layer. Lastly, when the volume of water in the sample increases, L-Arginine solution has no absorption peak but is covered by a large amount of scattered water. Therefore, the absorption spectrum of L-Arginine solution is almost the same as that of free water, which is closely related with the strong absorption of water.

Figure 4B shows the refractive index of L-Arginine crystal, L-Arginine hydrate, and L-Arginine solution. In order to fully present and analyze the refractive index trend, Figure 4B uses different coordinate ranges

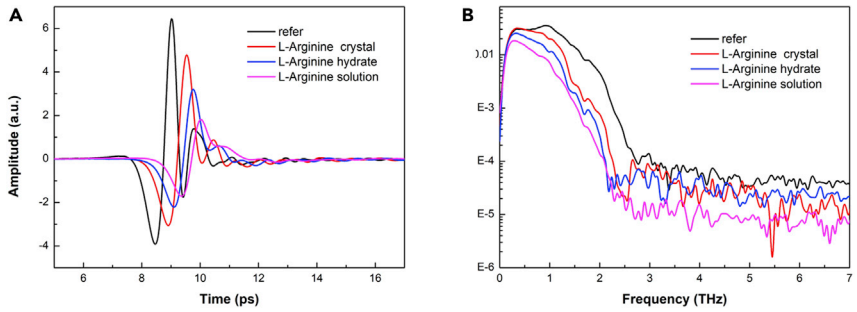

Figure 3. THz time-domain waveforms and spectra of reference, L-Arginine crystal, as well as its hydrate and aqueous solution

(A and B) (A) Time-domain waveforms; (B) the corresponding frequency-domain waveforms.

of double y axes to characterize the refractive index trend. We find that the refractive index of L-Arginine crystal and its hydrate have three peaks that are the same as the absorption spectrum. Also, the change in the trend of the refractive index with respect to the frequency is just opposite to the corresponding absorption spectrum. For L-Arginine solution, the refractive index is larger than that of its crystal and hydrate; its trend is different but consistent with that of free water.

Dielectric coefficient

An absorption characteristic spectrum is often used as the only feature vector for automatic tissue recognition, but owing to the complexity of tissues and cells, its reliability is slightly insufficient. A dielectric spectrum is a series of micro changes caused by the interaction between samples and THz waves. In addition, dielectric spectroscopy is very sensitive to the interaction between molecules and the structural changes inside the molecules. The structural information of the substance can be obtained through the relaxation process. Therefore, the dielectric constant is sensitive to molecular interaction and intramolecular structural changes. The dielectric coefficient is a complex number, where the real part is equivalent to the energy storage part, i.e., the absorbed part after the THz wave is input, whereas the imaginary part is equivalent to the loss part, which is consumed by the dielectric. Figures 5A and 5B show the real and imaginary parts of the dielectric coefficient of L-Arginine crystal, L-Arginine hydrate, and L-Arginine solution, respectively. It can be observed that the trend of the imaginary parts of L-Arginine crystal and its hydrate is completely consistent with their corresponding absorption spectrum, whereas the trend of their real parts is completely opposite to that of the imaginary part. The above results verify the accuracy of the absorption peaks of L-Arginine crystal and L-Arginine hydrate. Although the dielectric coefficients of L-Arginine solution do not conform to the law corresponding to its absorption spectrum, it is consistent with the law of dielectric characteristics of free water. Moreover, the dielectric response of L-Arginine solution is much higher than that of L-Arginine crystal and its hydrate. The reasons for this phenomenon may lie in that the complex permittivity of free water is divided into three modes: slow relaxation mode, fast relaxation mode, and molecular bond vibration (Raicu and Feldman, 2015). When a hydration layer is formulated by the combination of waterand solvent molecules, the dielectric response of these molecules may only

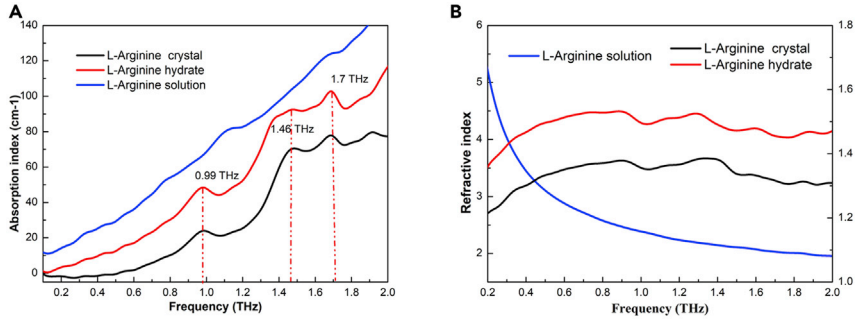

Figure 4. Characteristic spectra of L-Arginine crystal, as well as its hydrate and aqueous solution

(A and B) (A) Absorption index and (B) refractive index.

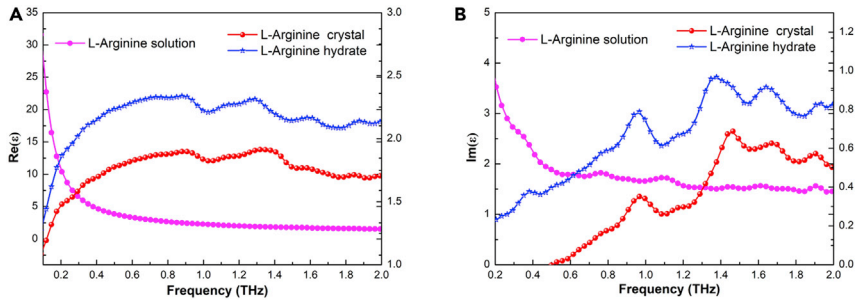

Figure 5. Dielectric coefficient of L-Arginine crystal, and its hydrate and solution
(A and B) (A) Real part and (B) imaginary part.

be related to the hydration state and the formation of a hydrogen bond network, whereas the absorption peak is caused only by the vibration of the solute molecule.

Conclusions

In this paper, the THz spectra of L-Arginine crystal as well as its hydrate and solution were measured directly. We obtained the absorption characteristic spectrum of the three involved L-Arginine samples in the range from 0.1 to 2.0 THz. It is found that (1) L-Arginine crystal and its hydrate have the same three absorption peaks, which are at 0.99, 1.46, and 1.7 THz, respectively; (2) L-Arginine solution and free water have the same trend of characteristic absorption spectrum; and (3) the absorption baselines of the three involved L-Arginine samples are different. Moreover, some THz spectral information (such as refractive index, real dielectric constant, and imaginary dielectric constant) is also analyzed and discussed in detail, which can be used to verify the reliability of the obtained fingerprint spectrum. The acquisition of these spectral information is significant to provide a reliable technical means for detecting the cells and tissues with hydration-sensitive lesions.

Limitations of the study

For the detection of L-Arginine solution, the absorption spectrum we obtained did not detect the absorption peak of solvent molecules. Is it because the strong absorption of water masks the absorption peak of the sample itself or the complex changes of sample molecules in the solution lead to the absence of the absorption peak? These can be further explored in the future.

STAR★METHODS

Detailed methods are provided in the online version of this paper and include the following:

- KEY RESOURCES TABLE
- RESOURCE AVAILABILITY
  - Lead contact
  - Materials availability
  - Data and code availability
- EXPERIMENTAL MODEL AND SUBJECT DETAILS
- METHOD DETAILS
  - Sample preparation
  - THz-TDS system
  - Calculations of optical parameters
- QUANTIFICATION AND STATISTICAL ANALYSIS
- ADDITIONAL RESOURCES

SUPPLEMENTAL INFORMATION

Supplemental information can be found online at https://doi.org/10.1016/j.isci.2022.103788.

ACKNOWLEDGMENTS

This work was supported in part by the National Key Research and Development Program of China (Grant No. 2017YFA0701005) and in part by the National Natural Science Foundation of China (Grant No.

51807161, 62075179). The author thanks Professor Hongwei Zhao for her contribution to sample preparation.

AUTHOR CONTRIBUTIONS

The academic idea of this paper was proposed by W.S. The experiment is guided by L.H. H.W. and Z.W. carried out the experimental work. M.W., Chaofan Li, and Chunhui Li conducted experiment records. The manuscript was written by W.S. and H.W.

DECLARATION OF INTERESTS

The authors declare no competing interests.

Received: September 14, 2021
Revised: December 15, 2021
Accepted: January 13, 2022
Published: February 18, 2022

REFERENCES

Bagchi, B. (2005). Water dynamics in the hydration layer around proteins and micelles. Chem. Rev. *105*, 3197–3219. https://doi.org/10.1021/cr020661+.

Biman, and Bagchi. (2005). Water dynamics in the hydration layer around proteins and micelles. Chem. Rev. *105*, 3197–3219. https://doi.org/10.1021/cr020661.

Doan, L.C., and Vinh, N.Q. (2020). Investigating hydration dynamics and protein collective motions by high-precision dielectric spectroscopy. Proc. SPIE *11499*, 114990O1-7. https://doi.org/10.1117/12.2567857.

Gupta, P.K., Esser, A., Forbert, H., and Marx, D. (2019). Toward theoretical terahertz spectroscopy of glassy aqueous solutions: partially frozen solute–solvent couplings of glycine in water. Phys. Chem. Chem. Phys. *21*, 4975–4987. https://doi.org/10.1039/C8CP07489E.

Heugen, U., Schwaab, G., Bründermann, E., Heyden, M., Yu, X., Leitner, D.M., and Havenith, M. (2006). Solute-induced retardation of water dynamics probed directly by terahertz spectroscopy. Proc. Natl. Acad. Sci. U S A *103*, 12301–12306. https://doi.org/10.1073/pnas.0604897103.

Hou, L., Shi, W., Dong, C., Yang, L., Wang, Y., Wang, H., Hang, Y., and Xue, F. (2021). Probing trace lactose from aqueous solutions by terahertz time-domain spectroscopy. Spectrochimica Acta A Mol. Biomol. Spectrosc. *246*, 119044. https://doi.org/10.1016/j.saa.2020.119044.

Liu, G., Chang, C., Qiao, Z., Wu, K., Zhu, Z., and Cui, G. (2019). Myelin sheath as a dielectric waveguide for signal propagation in the mid-infrared to terahertz spectral range. Adv. Funct. Mater. *29*, 1807862.1–1807862.6. https://doi.org/10.1002/adfm.201807862.

Markelz, A.G., Roitberg, A., and Heilweil, E.J. (2000). Pulsed terahertz spectroscopy of DNA, bovine serum albumin and collagen between 0.1 and 2.0 THz. Chem. Phys. Lett. *320*, 42–48. https://doi.org/10.1016/S0009-2614(00)00227-X.

Nagai, N., Kumazawa, R., and Fukasawa, R. (2005). Direct evidence of inter-molecular vibrations by THz spectroscopy. Chem. Phys. Lett. *413*, 495–500. https://doi.org/10.1016/j.cplett.2005.08.023.

Peng, Y., Shi, C., Zhu, Y., Gu, M., and Zhuang, S. (2020). Terahertz spectroscopy in biomedical field: a review on signal-to-noise ratio improvement. PhotoniX *1*, 1–18. https://doi.org/10.1186/s43074-020-00011-z.

Penkov, N., and Fesenko, E. (2020). Development of terahertz time-domain spectroscopy for properties analysis of highly diluted antibodies. Appl. Sci. *10*, 7736.

Pickwell, E., Cole, B.E., Fitzgerald, A.J., Pepper, M., and Wallace, V.P. (2004). In vivo study of human skin using pulsed terahertz radiation. Phys. Med. Biol. *49*, 1595–1607. https://doi.org/10.1088/0031-9155/49/9/001.

V. Raicu, and Y. Feldman, eds. (2015). Dielectric Relaxation in Biological Systems: Physical Principles, Methods, and Applications (Oxford University Press).

Shi, W., Wang, H.Q., Hou, L., Dong, C.G., Li, C.F., Yang, L., Zhao, H.W., Wang, Z.Q., and Wang, Y.Z. (2021). Terahertz spectral nondestructive detection of amino acid molecules in aqueous solution. Sci. Sin. Phys. Mech. Astron. *51*, 054210. https://doi.org/10.1360/SSPMA-2020-0279.

Shi, W., Wang, Y., Hou, L., Ma, C., Li, J., Dong, C., Wang, Z., Wang, H., Guo, J., Xu, S., et al. (2020). Detection of living cervical cancer cells by transient terahertz spectroscopy. J. Biophotonics *14*, e202000237. https://doi.org/10.1002/jbio.202000237.

Tang, M., Zhang, M.K., Xia, L., Yang, Z., and Cui, H.L. (2020). Detection of single-base mutation of DNA oligonucleotides with different lengths by terahertz attenuated total reflection microfluidic cell. Biomed. Opt. Express *11*, 5362–5372. https://doi.org/10.1364/BOE.400487.

Wang, R., Xu, L., Wang, J., Sun, L., Jiao, Y., and Meng, Y. (2021). Electric fano resonance-based terahertz metasensors. Nanoscale *13*, 18467–18472. https://doi.org/10.1039/D1NR04477J.

Woodward, R.M., Cole, B.E., Wallace, V.P., Pye, R.J., Arnone, D.D., Linfield, E.H., and Pepper, M. (2002). Terahertz pulse imaging in reflection geometry of human skin cancer and skin tissue. Phys. Med. Biol. *47*, 3853. https://doi.org/10.1088/0031-9155/47/21/325.

Xu, W., Xie, L., Zhu, J., Xu, X., Ye, Z., and Wang, C. (2016). Gold nanoparticle-based terahertz metamaterial sensors: mechanisms and applications. ACS Photon. *3*, 2308–2314. https://doi.org/10.1021/acsphotonics.6b00463.

Yang, K., Yang, X., Zhao, X., Lamy de la Chapelle, M., and Fu, W. (2018). THz spectroscopy for a rapid and label-free cell viability assay in a microfluidic chip based on an optical clearing agent. Analy. Chem. *91*, 785–791. https://doi.org/10.1021/acs.analchem.8b03665.

Yi, Z., Liu, Q., Xia, Y., Huang, H.C., and Zhu, L.G. (2017). Label-free monitoring of cell death induced by oxidative stress in living human cells using terahertz ATR spectroscopy. Biomed. Opt. Express *9*, 14. https://doi.org/10.1364/BOE.9.000014.

Zhang,C.,Liang,L.,Ding,L.,Jin,B.,Hou,Y.,Li,C.,Jiang,L., Liu,W.,Hu,W.,andWu,P.(2016).Label-free measurementsoncellapoptosisusingaterahertz metamaterial-basedbiosensor.Appl.Phys.Lett.*108*, 241105.https://doi.org/10.1063/1.4954015.

Zhu, Y., Shi, C., Wu, X., and Peng, Y. (2021). Terahertz spectroscopy algorithms for biomedical detection. Acta Opt. Sin *1*, 0130001. https://doi.org/10.3788/AOS202141.0130001.

STAR★METHODS

KEY RESOURCES TABLE

REAGENT or RESOURCE	SOURCE	IDENTIFIER
L- Arginine		
L-Arginine crystal	J&K Chemical	CAS#: 74-79-3
Software and algorithms		
Origin 8	Origin Lab	https://www.originlab.com/
Matlab R2014a	MathWorks	https://cn.mathworks.com/
Deposited data		
code	This paper	https://doi.org/10.5281/zenodo.5832524

RESOURCE AVAILABILITY

Lead contact

Further information and requests for resources and reagents should be directed to and will be fulfilled by the Lead Contact, Wei Shi (swshi@mail.xaut.edu.cn).

Materials availability

This study did not generate new unique reagents.

Data and code availability

All data reported in this paper will be shared by the lead contact upon request.

All original code has been deposited at Zenodo (Wang et al., 2022) and is publicly available as of the date of publication. DOI are listed in the key resources table.

Any additional information required to reanalyze the data reported in this paper is available from the lead contact upon request.

EXPERIMENTAL MODEL AND SUBJECT DETAILS

Our study does not use experimental models typical in the life sciences.

METHOD DETAILS

Sample preparation

We process a push-pull TPX sample cell, where the inner diameter is 7 mm and the groove depth is 100 μm Figure S1A is design diagram of THz liquid sample cell, and Figure S1B is the photos of push-pull TPX sample cell and preparation process of three types of samples involved L-Arginine. The purity of L-Arginine used during the experiment is of analytical purity. We divide samples into three types: *dry tablet*, *suspension*, and *dissolved solution*, according to the binding form of L-arginine and water molecules and the amount of dispersed water. Specifically, the dry anhydrous L-Arginine tablets are compacted in the sample cell with a thickness of 100 μm. The L-Arginine suspension is produced as follows: firstly, water is sprayed into the tablet to ensure that the sprayed water is fine and uniform. Since the thickness of the tablet is only 100um, the water can cover all the solid particles at once. Next, we use the cover of sample cell to push the high concentration suspension of L-Arginine, ensuring that no water was squeezed out and no free water was found outside the particles. Finally, the mass of the sample before and after water spraying is weighed by an analytical balance, and the mass concentration is calculated as 0.3 mg/mL. To formulate the saturated L-Arginine solution, L-Arginine powder is completely dissolved in distilled water, and the solution was filled into the sample cell as a mass concentration reached 0.0148 mg/mL.

THz-TDS system

We have built a THz-TDS system, and its overall optical path is shown in Figure 1. The whole system is mainly composed of femtosecond laser, THz radiation source (home-made GaAs antenna), testing platform, and THz detector. The femtosecond laser (MaiTai XF-1 titanium sapphire, Spectra-Physics) is used as the light source with the center wavelength of laser is 800 nm, the pulse width of about 80 fs, and the repetition frequency of 80 MHz. Femtosecond laser is divided into pump beam and probe beam by a 70/30 beam splitter (BS), and their pulse powers are set to 200 mW and 30 mW by two attenuators, respectively; the laser power is measured by optical energy meter (J-25 MB-LE, 25 J–50 MJ). As shown in the experimental setup, after reflected by M6 and M7, the pump beam is focused on a photoconductive antenna by a lens (L1) with the focal length of 100 mm, thus generating high-power terahertz pulses. THz pulses are collimated by the first off-axis parabolic mirror (OPM1), and then converged by the off-axis parabolic mirror (OPM2). Different L-Arginine samples are placed at the focus of the second off-axis parabolic mirror. The transmitted THz wave carrying the sample information is collected and focused on the ZnTe by OPM3 and OPM4. On the other hand, after passing through the delay system and reflected by M5, the probe beam transmits through the ITO film. Finally, the probe beam and THz wave are collinearly incident onto the ZnTe crystal along the vertical direction, and emergent light carries THz information of samples. Next, THz wave as well as the sample information is sent to a quarter-wave plate (QWP) followed by a Wollaston prism (WL). Another lens (L2) is placed before QWP to focus the probe beam onto a balanced detector. The output signal is sent to a lock-in amplifier and recorded by a computer, which can directly obtain sample information in THz frequency. The detection method of electro-optical sampling used in this experiment setup (see Figure S2) and the optical principle involved is the principle of equivalent time sampling (see Figure S3). With this information, the amplitude and phase in a certain spectrum range are obtained by Fourier transform, and the absorption coefficient, refractive index and dielectric constant of the samples are calculated.

Calculations of optical parameters

Optical parameters are important to study substances and materials. In particular, absorption coefficient, refractive index and dielectric constant are important physical parameters to describe substances. THz-TDS records the time-domain waveform of THz pulse, so the waveform through the sample contains all the optical information of the sample material.

The THz spectrum $F[E_0(t)]$ in free space is

$$F[E_0(t)] = E_0(\omega) = A_0(\omega)e^{i\varphi_0(\omega)} \quad \text{(Equation 1)}$$

Here, $A_0(\omega)$ and $\varphi_0(\omega)$ are the amplitude and phase of THz spectrum, respectively

The THz spectrum $F[E(t)]$ after passing through the sample is

$$F[E(t)] = E(\omega) = A_0(\omega).\mathrm{T}.FP.e^{i\varphi(\omega)} = A_0(\omega).\mathrm{T}.FP.e^{i\varphi_0(\omega)}e^{-\alpha(\omega)d}e^{i\frac{2\pi}{\lambda}(n-1)d} \quad \text{(Equation 2)}$$

Here, $\alpha(\omega)$ is the absorption coefficient of the sample, d and n are thickness and refractive index of the sample, respectively. $T_{1\to2}$ is the accumulation of amplitude propagation coefficient caused by the interface of two substances. For two substances with refractive index n_1 and n_2, their values are determined by Fresnel equation

$$T_{1\to2} = \frac{2n_2}{n_1 + n_2} \quad \text{(Equation 3)}$$

FP is the accumulation of Fabry Perot effect factors and represents the superposition term of multiple reflection of THz wave in various media.

Bring the samples with thickness d_1 and d_2 into Equation 2, respectively

$$E_1(\omega) = A_1(\omega).\mathrm{T}_1.FP_1.e^{i\varphi_1(\omega)} = A_0(\omega).\mathrm{T}_1.FP_1.e^{i\varphi_0(\omega)}e^{-\alpha(\omega)d_1}e^{i\frac{2\pi}{\lambda}(n-1)d_1} \quad \text{(Equation 4)}$$

$$E_2(\omega) = A_2(\omega).\mathrm{T}_2.FP_2.e^{i\varphi_2(\omega)} = A_0(\omega).\mathrm{T}_2.FP_2.e^{i\varphi_0(\omega)}e^{-\alpha(\omega)d_2}e^{i\frac{2\pi}{\lambda}(n-1)d_2} \quad \text{(Equation 5)}$$

For samples with only different thickness, the interface of THz wave and Fabry Perot effect are the same, so $T_1 = T_2$, $FP_1 = FP_2$. Assuming $d_1 < d_2$, with thin samples as reference, there is

$$\frac{E_2(\omega)}{E_1(\omega)} = \frac{A_2(\omega)}{A_1(\omega)} e^{i(\varphi_2(\omega)-\varphi_1(\omega))} = e^{-\alpha(\omega)(d_2-d_1)} e^{i\frac{2\pi}{\lambda}(n-1)(d_2-d_1)} \quad \text{(Equation 6)}$$

The amplitude is compared by Equation 6, and the absorption coefficient $\alpha(\omega)$ is

$$\alpha(\omega) = -\log_{10}(A(\omega)/A_0(\omega))/(d_2-d_1) \quad \text{(Equation 7)}$$

By comparing the phase with Equation 6, the refractive index n is

$$n = \frac{c(\varphi_1(\omega)-\varphi_0(\omega))}{\omega d} + 1 \quad \text{(Equation 8)}$$

The extinction coefficient $k(\omega)$ describes the loss of electromagnetic wave propagation in dielectric, which can be directly calculated from the absorption coefficient $\alpha(\omega)$:

$$k(\omega) = \frac{\alpha(\omega)c}{4\pi\omega} \quad \text{(Equation 9)}$$

The dielectric constant ε of the sample is:

$$\varepsilon = \varepsilon'(\omega) + i\varepsilon''(\omega) \quad \text{(Equation 10)}$$

By refractive index $n(\omega)$ And extinction coefficient $k(\omega)$, The real parts $\varepsilon'(\omega)$ and imaginary parts $\varepsilon''(\omega)$ of the dielectric constant can be directly derived, and the relationship is as follows:

$$\varepsilon'(\omega) = n^2(\omega) - k^2(\omega) \quad \text{(Equation 11)}$$

$$\varepsilon''(\omega) = 2n(\omega)k(\omega) \quad \text{(Equation 12)}$$

QUANTIFICATION AND STATISTICAL ANALYSIS

There is no statistical analysis in this paper

ADDITIONAL RESOURCES

We have no relevant resources.